Author Manuscript

Faculty of Biology and Medicine Publication

This paper has been peer-reviewed but does not include the final publisher proof-corrections or journal pagination.

Published in final edited form as:

Title: Contributions of Intraindividual and Interindividual Differences to Multisensory Processes.

Authors: Murray MM, Thelen A, Ionta S, Wallace MT

Journal: Journal of cognitive neuroscience

Year: 2018 Feb 28

Pages: 1-17

DOI: 10.1162/jocn$_{a0}$1246

Journal of
Cognitive Neuroscience

Contributions of intra- and inter-individual differences to multisensory processes

Journal:	*Journal of Cognitive Neuroscience*
Manuscript ID	JOCN-2017-0185.R1
Manuscript Type:	Original
Date Submitted by the Author:	29-Nov-2017
Complete List of Authors:	Murray, Micah; The Laboratory for Investigative Neurophysiology, Department of Clinical Neurosciences and Department of Radiology, Vaudois University Hospital Center and University of Lausanne; Centre Hospitalier Universitaire Vaudois and University of Lausanne, Electroencephalography Brain Mapping Core, Center for Biomedical Imaging; The Department of Ophthalmology, Jules Gonin Eye Hospital and University of Lausanne; Department of Hearing and Speech Sciences, Vanderbilt University Medical Center Thelen, Antonia; Vanderbilt University Brain Institute Ionta, Silvio; The Laboratory for Investigative Neurophysiology, Department of Clinical Neurosciences and Department of Radiology, Vaudois University Hospital Center and University of Lausanne; Rehabilitation Engineering Laboratory, Department of Health Sciences and Technology, ETH Zürich Wallace, Mark; Vanderbilt University Brain Institute; Kennedy Center for Research on Human Development, Vanderbilt University; Department of Psychiatry, Vanderbilt University
Keywords:	EEG, Multisensory, Perception: Multisensory processing

Contributions of intra- and inter-individual differences to multisensory processes

Micah M. Murray[1-4,†], Antonia Thelen[5,†], Silvio Ionta[1,3,6], and Mark T. Wallace[4,5,7-9†]

[1]The Laboratory for Investigative Neurophysiology (The LINE), Department of Clinical Neurosciences and Department of Radiology, Vaudois University Hospital Center and University of Lausanne, Lausanne 1011, Switzerland
[2]Electroencephalography Brain Mapping Core, Center for Biomedical Imaging of Lausanne and Geneva, Lausanne 1011, Switzerland
[3]The Department of Ophthalmology, Fondation Asile des Aveugles and University of Lausanne, Lausanne 1003, Switzerland
[4]Department of Hearing and Speech Sciences, Vanderbilt University Medical Center, Nashville, TN, USA
[5]Vanderbilt Brain Institute, Vanderbilt University, Nashville, TN 37203-5721, USA
[6]Rehabilitation Engineering Laboratory, Department of Health Sciences and Technology, ETH Zürich 8092, Zürich, Switzerland
[7]Kennedy Center for Research on Human Development, Vanderbilt University, Nashville, TN 37203-5721, USA
[8]Department of Psychiatry, Vanderbilt University, Nashville, TN 37203-5721, USA
[9]Department of Psychology, Vanderbilt University, Nashville, TN 37203-5721, USA

† denotes equal contributions

***Address correspondence to:**
Prof. Micah Murray
Centre Hospitalier Universitaire Vaudois
Radiology, BH08.078
Rue du Bugnon 46
1011 Lausanne Switzerland
e-mail: micah.murray@chuv.ch

Abstract

Most evidence on the neural and perceptual correlates of sensory processing derives from studies that have focused on only a single sensory modality and averaged the data from groups of participants. Although valuable, such studies ignore the substantial inter- and intra-individual differences that are undoubtedly at play. Such variability plays an integral role in both the behavioral/perceptual realms and in the neural correlates of these processes, but substantially less is known when compared with group-averaged data. Recently, it has been shown that the presentation of stimuli from two or more sensory modalities (i.e., multisensory stimulation) not only results in the well-established performance gains, but also gives rise to reductions in behavioral and neural response variability. To better understand the relationship between neural and behavioral response variability under multisensory conditions, the present study investigated both behavior and brain activity in a task requiring subjects to discriminate moving versus static stimuli presented in either a unisensory or multisensory context. Electroencephalographic (EEG) data were analyzed with respect to intra- and inter-individual differences in reaction times (RTs). The results showed that trial-by-trial variability of RTs was significantly reduced under audiovisual presentation conditions as compared to visual-only presentations across all participants. Intra-individual variability of RTs was linked to changes in correlated activity between clusters within an occipital to frontal network. Additionally, inter-individual variability of RTs was linked to differential recruitment of medial frontal cortices. The present findings highlight differences in the brain networks that support behavioral benefits during unisensory vs. multisensory motion detection, and provide an important view into the functional dynamics within neuronal networks underpinning intra-individual performance differences.

Introduction

A large body of work has focused its effort on disentangling the general principles underlying perceptual processes (and ultimately behavior). Much of this work has focused on reporting behavioral and/or neurophysiological findings that result from group-averaged data analysis approaches (for reviews see: Grill-Spector, 2003; Peelen & Downing, 2007; Pulvermüller & Fadiga, 2010; Schmid & Maier, 2015). Although such group-average analyses represent a necessary initial step, they often fail to address the enormous (and important) variability that characterizes performance both within and across individuals (Dickman, 1985; Witkin, 1949, 1950). The importance of inter-individual differences is evident in behavior, perception and cognition (for reviews see: Kanai & Rees, 2011; Kane & Engle, 2002). In addition to inter-individual variability, substantial intra-individual variability is a hallmark of many sensory, perceptual, and cognitive processes (Castellanos et al., 2005; Fiske & Rice, 1955; MacDonald, Nyberg, & Bäckman, 2006; Morell & Morell, 1966; Simmonds et al., 2007). An exemplar account of such trial-by-trial fluctuations in regards to sensory processing was provided by Dehaene (1993). The author reported a periodic structure to the distribution of reaction times (RTs) in a series of auditory and visual discrimination tasks (Dehaene, 1993). The stochastic nature of the RT distributions suggested inter-trial fluctuations in the accumulation of sensory information and/or response generation. More recently, these trial-to-trial changes in performance have been linked to differences in state-dependent neural processing that in turn cascade into differences in the processing time of perceptual information (e.g. Bourgeois, Chica, Valero-Cabré, & Bartolomeo, 2013; Corbetta & Shulman, 2002). Additional evidence has been gathered regarding the neurophysiological mechanisms that may support these intra-individual differences (e.g. Chaumon & Busch, 2014; Romei, Gross, & Thut, 2010; de Graaf et al., 2013). One example is that trial-to-trial differences in the magnitude and latency of evoked gamma band responses (eGBR) can predict variability in response speed in visual detection tasks (Fründ, Busch, Schadow, Körner, & Herrmann, 2007).

While these studies have produced important insights into the functional mechanisms underpinning intra-individual variability, lesion and hemodynamic imaging studies have provided additional evidence on the neuronal architecture supporting such variability. For example, lesions to frontal cortices, right inferior parietal cortex and regions of the thalamus can result in increased variability in intra-individual reaction time (RT) (Bellgrove, Hester, & Garavan, 2004; Stuss, Floden, Alexander, Levine, & Katz, 2001; Stuss et al., 2003). In a reexamination of neuroimaging data across a broad range of visual experimental tasks, Yarkoni and colleagues reported evidence for an extended network including visual cortices as well as cerebellum and additional subcortical structures to be related to RT variability (Yarkoni, Barch, Gray, Conturo, & Braver, 2009). Collectively, these studies have revealed a highly distributed network of brain regions that appears to play a role in trial-to-trial response variability, with a specific emphasis on RTs.

Although highly revealing as to the characteristics of inter- and intra-individual variability at both the behavioral and neural levels, it is important to note that these studies have largely been focused within a single sensory system – vision. As an extension of this work, there is a growing body of evidence showing both perceptual benefits and reduced behavioral variability when multiple redundant signals are presented within a single sensory modality (e.g., two redundant visual targets) (Los & Van der Burg, 2013; Miller, 1982; Pérez-Bellido, Soto-Faraco, & López-Moliner, 2013). However, even under these unisensory redundant signal presentation conditions, substantial intra-individual response variability still exists (Iacoboni & Zaidel, 2003; Ivanov & Werner, 2009; Krummenacher, Grubert, Töllner, & Müller, 2014; Martuzzi et al., 2006; Miniussi, Girelli, & Marzi, 1998; Murray, Foxe, Higgins, Javitt, & Schroeder, 2001; Saron, Schroeder, Foxe, & Vaughan, 2001).

Under naturalistic circumstances, sensory information about an event is frequently conveyed through multiple sensory systems. Take as an example a bouncing ball, and in which the visual and auditory cues provide complementary information about the ball's collision with the floor. Under such multisensory conditions, intra-individual response variability can be significantly reduced when compared with unisensory presentation conditions (reviewed in Murray & Wallace, 2011). Moreover, these investigations have provided robust evidence of significant decreases in variability of behavioral and neurophysiological responses to occur under multisensory presentation conditions, which exceed those observed under redundant unisensory trials (e.g. Gingras, Rowland, & Stein, 2009). Despite a growing number of circumstances in which such multisensory redundancy-mediated reductions in performance variability have been demonstrated, the neural correlates of these effects remain poorly understood. The aim of the current study was to address this open question.

Several studies have provided some insight into this issue, and have shown that multisensory presentations that result in fast RTs are accompanied by increased power and phase coherence within early, low-level sensory cortices (Altieri, Stevenson, Wallace, & Wenger, 2015; Mercier et al., 2015; Senkowski, Molholm, Gomez-Ramirez, & Foxe, 2006; Sperdin, Cappe, Foxe, & Murray 2009). While these data provide some information about the temporal dynamics underpinning RT variability under multisensory conditions, hemodynamic imaging has provided additional insight into the important nodes in a putative network. For example, Noppeney and colleagues (2010) found activity within a widespread network, spanning occipital to frontal cortices, to be modulated by both the ambiguity of the auditory and visual stimuli as well as their congruency in a visual object categorization task. Moreover, these authors provided evidence that this network activation is linked to the efficacy of the behavioral responses observed (Noppeney, Ostwald, & Werner, 2010). Taken together, these previous studies provide a base of knowledge regarding the functional mechanisms and neuronal structures involved in response variability under multisensory presentations. Nonetheless, much remains to be elucidated, most notably how trial-by-trial changes in activity within the associated network(s) give rise to the striking variability observed in behavioral performance.

To this aim, in the current study, we re-analyzed previously published ERP data (Cappe, Thelen, Romei, Thut, & Murray, 2012). The initial study had been designed to investigate the neuronal mechanisms involved in the selective response facilitation observed under multisensory conditions for the detection of approaching (i.e., looming) versus receding motion cues. Specifically, subjects were asked to detect motion under unisensory (auditory or visual-only) and multisensory (audiovisual) presentation conditions. The present analysis specifically focused on determining the neuronal networks underlying the RT variability that accompanies behavioral performance on this task.

Materials and Methods

Subjects

After applying criteria for the minimal number of accepted trials per condition (detailed below), the data from eight healthy individuals were included in the current analyses (aged 18-28yrs: mean = 23±3yrs; 3 women and 5 men; 7 right-handed). All subjects reported normal hearing and normal or corrected-to-normal vision. Handedness was assessed with the Edinburgh questionnaire (Oldfield, 1971). None of the subjects reported a history of neurological or psychiatric illness. Participants provided written, informed consent to the procedures that were approved by the Ethics Committee of the Faculty of Biology and Medicine of the University Hospital and University of Lausanne.

Stimuli and procedure

We performed quartile-by-quartile analysis on a previously published dataset (Cappe et al., 2012). A quartile analysis was chosen because inter-quartile range (IQR) is considered a robust measure of the spread of data, particularly when they are non-normally distributed as if often the case for reaction time data from individual participants (Ratcliffe, 1993). Only the features relevant to the quartile-by-quartile analysis will be detailed here. Briefly, participants were asked to perform a speeded detection task, and were asked to indicate the presence of moving versus static stimuli by a simple button press. Stimuli could be presented in a unisensory (i.e. visual or auditory only) or multisensory (i.e. audiovisual) manner. Visual and auditory motion was perceived as either approaching or receding from the observer. Additionally, the original design included static stimuli in both modalities. The experiment was composed of 15 conditions, consisting of 6 unisensory (auditory (A) and visual (V) only, static (s), receding (r) or approaching (looming=l) stimuli) and 9 multisensory pairings (the full set of possible auditory-visual (AV) combinations). Overall, we collected 252 trials for each condition over 18 blocks. In anticipation of our analysis strategy, comparing predicted versus empirically derived cumulative distribution functions (CDFs; see Methods section for Behavioral data), we here only considered multisensory stimuli that were composed of a combination of two unisensory motion cues (VlAl, VlAr, Vr, AL, VrAr, and their respective unisensory components: Vl, Vr, Al, Ar).

Visual motion stimuli consisted of a disc (initial size: 7° of visual angle) dynamically contracting (to 1°) or expanding (to 13°) over 500ms of stimulus duration. Auditory stimuli consisted of 1000Hz complex pure tones (44.1kHz sampling; 500ms duration; 10ms rise/fall to avoid clicks), composed of triangular waveforms. To induce the perception of motion, the amplitude of the stimuli was linearly modulated (77 ± 10dB SPL) over the stimulus duration period. After stimulus offset, a variable inter-trial-interval of 800-1400ms was interleaved such that the onset of the next trial could not be anticipated by subjects. Additionally, all audiovisual stimulus pairings were presented synchronously. Stimulus delivery and response recording were controlled by E-Prime in conjunction with their Serial Response Box (Psychology Software Tools; www.pstnet.com).

Data Acquisition

Concurrently to the behavioral task, we acquired continuous high-density (160-channel-BioSemi ActiveTwo; www.biosemi.com) EEG at 1024Hz. The low-impedance AD-box references the data online to the common mode sense (CMS; active electrode), while grounding the data to the driven right leg (DRL; passive electrode). This functions as a feedback loop, driving the average instantaneous potential over the whole montage to the amplifier zero (for a more detailed description of the setup see: (http://www.biosemi.com/faq/cms&drl.htm).

Data Processing and Analyses

The aim of the current study was to investigate the neuronal correlates underpinning intra-individual RT variability observed at the behavioral level. To this end, only task-relevant conditions requiring subjects to respond to either sensory modality were included in the analyses (Vl, Vr, Al, Ar, VlAl, VrAr, VrAl, VlAr). To investigate the neuronal networks underpinning response speed variability, we ranked RT data for each of these eight conditions separately into four quartiles and calculated the mean response speed for each bin. Further, the present analyses sought to assess the neuronal networks underpinning multisensory benefits of behavioral responses over unisensory events. To this end, behavioral and EEG data were subsequently averaged across conditions, leading to three grand averages independently of motion direction (A, V, AV). In what follows, we only considered trials where RTs fell within the first and last of the quartiles, in order to compare behavioral and neuronal responses upon the fastest and slowest trials within each subject. Consequently, the data analyses carried out here specifically tested 1) differential processing under unisensory versus multisensory presentations and its' impact on behavior, and 2) the neural correlates underpinning response variability in terms of RTs.

Behavioral data

Intra-individual effects

To assess the occurrence of multisensory facilitation, response accuracy and reaction times were initially computed for each condition, separately. Race models were calculated to evaluate the occurrence of redundant signal effects (RSEs) under multisensory versus unisensory conditions (Ulrich & Miller, 1997; Ulrich, Miller, & Schröter, 2007). The race model assumes that auditory and visual information is processed independently upon multisensory presentations, and that responses are triggered by the faster unisensory process. Therefore, cumulative distribution functions (CDFs) of RTs for multisensory events can be computed based on the observed unisensory CDFs. These multisensory CDF predictions are then compared to the empirical CDFs from the observed RTs. If the empirical CDFs show significantly faster RTs for 20-50% of the percentiles, this is considered as race model violation and suggests that multisensory information was integrated prior to motor response initiation (Miller & Ulrich, 2003). Note, however, that neural integration can occur in the absence of evidence for race model violation in behavioral data (Murray et al., 2001).

Inter-individual effects and response facilitation

In addition to investigating the response variability within subjects, and across conditions, we also addressed how individual differences in response variability affect neuronal processing. To this end, we computed the difference in response speed between the mean RTs within the first and the last quartile for each subject and each condition (i.e. the IQR). IQRs have been considered a more robust quantification of the width of RT distributions as compared to central tendency measures, such as standard deviations, due to the fact that these distributions are non-normal by nature (see Ratcliff, 1993 for further detail). Thus, the index chosen here reflects the width of the individual response distributions, and serves as descriptor of the response variability for each subject.

Furthermore, this RT difference also served as a variable when directly testing the assumption that RT distributions were narrowed rather than broadened under multisensory conditions as compared to unisensory conditions. In recent years, there has been a debate as to whether RT distributions are skewed or broadened under multisensory as compared to unisensory presentation conditions (see Otto, Dassy, & Mamassian, 2013). Although not the central focus of the present study, our data contribute to the resolution of this debate by providing evidence that RT distributions are significantly skewed, rather than broadened, under multisensory presentation conditions.

EEG data preprocessing

EEG data were imported into MATLAB (http://www.mathworks.com), and preprocessing was performed using functions derived from the free EEGLAB toolbox and its ERPLAB plug-in (Delorme & Makeig, 2004; Lopez-Calderon & Luck, 2014). After import, a conventional 40Hz FIR low-pass filter was applied to the data. Subsequently, epochs from 200ms pre-stimulus to 700ms post-stimulus onset were extracted for each of the experimental conditions and from each subject to calculate ERPs. Epochs containing ±80μV artifacts, eye blinks or other noise transients were rejected by trial-by-trial visual inspection. Remaining epochs were binned according to RTs into fast (first quartile of the RT distribution) and slow (last quartile of the RT distribution) trials, and single-subject averages were computed for each condition separately. The single-subject ERPs were then exported to CARTOOL (Brunet, Murray, & Michel, 2011; https://sites.google.com/site/cartoolcommunity/files) for further processing. Data at artifact electrodes were interpolated using 3-D splines before creating the single-subject supra-condition averages (Perrin, Pernier, Bertrand, Giard et al., 1987). Baseline-corrected group averaged ERPs were computed over 100ms pre-stimulus to 600ms post-stimulus onset. When calculating ERPs, we equated the number of trials from the various contributing stimulus pairings, in the case of AV trials, and the number of artifact-free trials from each quartile. These criteria resulted in the exclusion of data from 6 of the original 14 participants because a reliable ERP was not evident upon visual inspection of their data after equating the number of trials.

General ERP Analysis Framework

Differences in neuronal activity were identified within an electrical neuroimaging framework, implemented in a variety of freeware and toolboxes (CarTool: Brunet et al., 2011; RAGU: Koenig, Kottlow, Stein, & Melie-García, 2011); STEN toolbox developed by Jean-François Knebel (http://www.unil.ch/line/home/menuinst/about-the-line/software--analysis-tools.html). This particular framework allows us to differentiate between modulations in response strength (GFP) and/or configuration (topography of the electric field) of neuronal networks recruited between conditions (for a review see Murray, Brunet, & Michel, 2008). Ultimately, we estimated and statistically assessed the neuronal sources involved, by using the local auto-regressive average distributed linear inverse solution (LAURA; Michel et al., 2004).

Lastly, in order to further investigate the neuronal correlates of inter-individual differences of response variability (i.e. differences in the spread of RTs between subjects), we submitted the data to an additional ANCOVA design, using the IQR as a covariate.

ERP waveform modulations

In a first step, we entered ERPs into a repeated-measures ANOVA, in order to analyze the waveforms from all electrodes as a function of time post-stimulus onset. We specifically tested for differences due to response speed (i.e. first versus forth quartile) and possible interactions with condition (i.e. A, V, AV). Temporal auto-correlation at the level of individual electrodes was corrected by applying a threshold criterion of ≥11 consecutive data-points (~11ms) (Guthrie & Buchwald, 1991). Additionally, only effects present at >5% of channels (i.e. ≥8) were considered reliable. This was implemented as a way to account for spatial correlation, which also varies as a function of time and thus cannot be set a priori. This mass univariate analysis of voltage waveforms was chosen to provide an overview of the spatiotemporal dynamics and distribution of the statistical effects. We emphasize that our analyses of interest were those based on reference-independent and global measures of the electric field at the scalp. Because these are global measures, no correction for spatial correlation was necessary.

Additionally, the analyses of voltage ERP waveforms at each electrode revealed a minimal influence of auditory ERPs to the overall observed statistical results pattern. Thus, although the full experimental design including auditory trials was considered throughout the analyses, we re-analyzed and focused the present report on results derived from a 2×2 ANOVA design, with the factors of response speed (fast, slow) and condition (V, AV). This approach led to the added advantage of increasing the observed effect sizes, by reducing the number of factors considered in our statistical analyses.

Electrical Neuroimaging

As mentioned above, analyses of ERP voltage waveforms are reference-dependent, with the consequence that statistical effects (and interpretations thereof) will also depend on the choice of the reference location (Murray et al., 2008). Consequently, our analyses focus instead on reference-independent global measures of ERP strength and topography that were analyzed within a so-called electrical neuroimaging framework (Michel & Murray, 2012). The first measure is global field power (GFP), which is the root mean square of the voltage data across the scalp (Lehmann & Skrandies, 1980). GFP is larger for stronger ERPs, but provides no information about the spatial distribution of the ERP. Here, GFP was analyzed with a 2×2 ANOVA using within-subject factors of RT speed (fast vs. slow trials) and condition (V vs. AV). ANOVA was performed on a millisecond-by-millisecond basis. Correction for temporal auto-correlation was achieved by considering as reliable only those effects lasting for at least 11 consecutive data-points (~11ms) (Guthrie & Buchwald, 1991). The second global measure is global dissimilarity (DISS), which is the root mean square of the difference between two GFP-normalized vectors (Lehmann & Skrandies, 1980). DISS can be analyzed in a factorial design using the Randomization Graphical User interface (RAGU) (König et al., 2011). Furthermore, in an additional ANCOVA design, we tested the impact of individual behavioral response variability, quantified here as the IQR for each experimental condition, on brain responses to the AV and V conditions leading to slow and fast reaction times. Subsequently, significant effects were assessed by submitting the data to post-hoc t-tests.

A topographic clustering analysis was also performed on the four group-averaged ERPs using CarTool. Specifically, we applied an atomize and agglomerate hierarchical clustering (AAHC) approach that uses measures of global explained variance alongside spatial correlation (see Murray et al., 2008 and Brunet et al., 2011 for detailed descriptions of the methods). By way of summary, topographic clustering is a data-driven and largely assumption-free means for identifying the minimal number of ERP topographies that explains a maximum of variance in the cumulative dataset (here the four group-averaged ERPs). Once this set of topographies and their sequence in time post-stimulus onset was identified, they were used as template maps for the fitting to single-subject ERPs. This fitting is based on the spatial correlation between a given template map and the single-subject ERP at a given moment post-stimulus for each condition and RT speed. As output, the fitting procedure yields the total amount of time a given template map was associated with responses to a given condition and/or RT speed.

Source Estimations

We estimated the neuronal sources of the electrical activity measured at the level of the scalp using a distributed linear inverse solution (minimum norm) together with the LAURA regularization approach (Grave de Peralta Menendez, Gonzalez Andino, Lantz, Michel, & Landis, 2001; Grave de Peralta Menendez, Murray, Michel, Martuzzi, & Gonzalez Andino, 2004; Michel et al., 2004). LAURA selects the source configuration that best mimics the biophysical behavior of electric vector fields (i.e. according to electromagnetic laws, activity at one point depends on the activity at neighboring points). In our study, homogenous regression coefficients in all directions and within the whole solution space were used. LAURA uses a realistic head model, and the solution space included 3005 nodes, selected from a 6x6x6mm grid of equally distributed nodes within the gray matter of the Montreal Neurological Institute's average brain (courtesy of R. Grave de Peralta and S. Gonzalez Andino; http://www.electrical-neuroimaging.ch/). Prior basic and clinical research from members of our group and others has documented and discussed in detail the spatial accuracy of the inverse solution model used here (e.g. Gonzalez Andino, Murray, Foxe, & de Peralta Menendez, 2005; Martuzzi et al., 2009; Michel et al., 2004).

The results of the above topographic pattern analysis defined time periods for which intra-cranial sources were estimated and statistically compared between conditions (here 183–250ms post-stimulus). Prior to calculation of the inverse solution, the ERPs were down-sampled and affine-transformed to a common 111-channel montage. Statistical analyses of source estimations were performed on a single average data point over the 183-250ms post-stimulus onset epoch. This procedure increases the signal-to-noise ratio of the data from each participant. The inverse solution was then estimated for each of the 3005 nodes. Consequently, the data were entered into a two-by-two ANOVA with the factors of response speed (i.e. fast versus slow trials) and condition (i.e. AV, V). Additionally, the data were submitted to an ANCOVA, using the difference in RTs between the first and the forth quartile as a covariate for each condition. Statistical results were corrected using a spatial extent criterion of at least 12 contiguous significant nodes. This spatial criterion was determined using the AlphaSim program (available at http://afni.nimh.nih.gov) and assuming a spatial smoothing of 2 mm FWHM and cluster connection radius of 8.5 mm. After 10000 Monte Carlo iterations, a cluster of 10 nodes was observed with a probability of 0.034, yielding a corresponding node-level p-value of $p \leq 0.001$ (see Sperdin, Cappe, & Murray, 2010; Thelen et al., 2012; Toepel, Knebel, Hudry, le Coutre, & Murray, 2009 for similar criteria). Results have been rendered on the Montreal Neurologic Institute's average brain with the Talairach & Tournoux (1988) coordinates of the largest statistical differences within each cluster indicated.

Cluster Correlations

In a last exploratory step, we investigated the relationship between activity within a left lateralized occipital cluster and the activity between the clusters identified by the main effect of quartile (i.e. fast versus slow RTs) in order to shed light upon the neuronal network interactions underpinning our results. This was predicated by a recent hemodynamic study by Noppeney et al. (2010), which revealed a linear relationship between activity within visual and frontal areas and trial-by-trial response efficacy (Noppeney et al., 2010).

To extract the activity within the most prominent occipital cluster while minimizing the contribution of weakly responsive sources, we only considered nodes with current density values exceeded two standard deviations above the whole brain volume's mean in each condition (here, mean + 2SD: Vslow=0.0008 + 0.0011µA/mm^3; Vfast=0.0008 + 0.0012µA/mm^3; AVslow=0.0008 + 0.001µA/mm^3; and AVfast=0.0007 + 0.001µA/mm^3; see Thelen et al., 2012 for a similar procedure). A cluster within left visual cortices extending to middle temporal cortex (MTG) was identified showing the strongest activations during the 183ms - 250ms post-stimulus onset period in all conditions (coordinates of nodes with maximum CSD values: Vslow=-48, -61, 1mm; Vfast/AVslow/AVfast=-49, -67, 6mm; MTG, BA37). No further nodes exceeding our statistical threshold were found.

Consequently, mean current density values for the cluster within the occipital cortex and each of the clusters yielding a main effect of RT quartile were extracted (i.e. first versus last quartile of the response distribution). More precisely, the mean activity across all voxels within three separate clusters, situated within the left Inferior Frontal Gyrus, the right Angular Gyrus/MTG, right Inferior Parietal Lobule (see Results for further details) were considered. We then 1) correlated the mean activity within each of these clusters with the activity within the occipital cluster and 2) the mean activity of between each of the three clusters as a function of time. Although we are hesitant to over interpret correlational relationships between activity patterns, this approach can at least reveal the basic interactions within a functional network. Given the small sample size, we used Spearman’s non-parametric rank-ordered correlation coefficient and a bootstrapping procedure with 2000 iterations to assess statistical reliability.

Results

*Behavioral dat*a

For the original analyses of the RT data, we refer readers to the previously published manuscript (Cappe et al., 2009). In the current study, we replicate the central behavioral result of speeded RTs under combined audiovisual stimulation, even with the smaller sample size dictated by the EEG analyses (significant main effect of condition $F_{(2, 6)}$=43.898; p<0.001; η_p^2=1; Post-hoc *t*-test confirming faster RTs to audiovisual presentations; median ± SEM: AV=427 ± 30ms; V=473 ± 20ms; A=624 ± 28ms; AV versus V: $t_{(7)}$=-2.532; p=0.039; AV versus A: $t_{(7)}$=-9.823; p<0.001; see Figure 1a).

We first sought to determine whether the audiovisual response speeding exceeded race model predictions (Ulrich & Miller, 1997; Ulrich et al., 2007). To this end, we modeled multisensory cumulative density functions (CDFs) based on the empirically derived unisensory CDFs and compared these to the empirically derived multisensory CDFs. We then entered the data from the modeled and the empirically derived multisensory CDFs into a repeated-measures ANOVA with the factors of data type (empirical versus modeled) and CDF percentile. This analysis revealed a main effect of percentile ($F_{(5,3)}$=142.5; p=0.001; η_p^2=1), and a significant data type by percentile interaction ($F_{(5,3)}$=9.6; p=0.046; η_p^2=0.66). Subsequently, we performed post-hoc one-tailed *t*-tests on each percentile, which revealed significant race model violations for trials within the first ~40 percentiles (p=0.026). Note that 1-tailed tests were conducted as we specifically tested for facilitation beyond race model predictions (i.e. a unidirectional effect). Furthermore, we divided the RT distributions into the fastest (first) and slowest (last) quartiles. Figure 1b plots the median RTs for the first and the last quartiles on the right of the CDFs. This figure illustrates the main effect of quartile ($F_{(1,7)}$=142.919; p<0.001; η_p^2 =1), the main effect of condition ($F_{(2,6)}$=47.649; p<0.001; η_p^2=1), and the condition by quartile interaction ($F_{(2,6)}$=8.627; p=0.017; η_p^2=0.816).

In a final step of the behavioral analyses, in order to assess response variability between conditions and at the inter-individual level, we computed the RT difference between the means of the first and the fourth quartiles for each condition and for the group (Figure 2a) and for each subject (i.e., approximation of the Inter Quartile Range; see Figure 2b). The one-way ANOVA on these RT difference scores revealed a significant main effect of condition ($F_{(2,6)}$=8.51; p=0.018; η_p^2=0.81) (Figure 2a). Post-hoc *t*-tests showed that the difference score for audiovisual RTs was significantly less variable than for either the visual or auditory conditions (median difference score ± SEM: AV=227 ± 21.6ms; V=261 ± 24.2ms; A=428 ± 50.5ms; AV versus V: $t_{(7)}$=-2.441, p=0.045; AV versus A: $t_{(7)}$=-4.106, p=0.005). Additionally, the difference score for visual RTs was significantly less variable than for auditory RTs ($t_{(7)}$=-3.443, p=0.011). Together, the behavioral data strongly support the presence of reduced variability under redundant (audiovisual) presentation conditions.

ERP data

ERP analyses were structured in order to reveal the neuronal networks underlying response variability observed at the behavioral level. Thus, we will refrain from reporting statistical differences between conditions (i.e., audiovisual vs. visual-only) since non-linear multisensory interactions were not the focus of the present manuscript (i.e. as compared to analyses presented by Sperdin et al., 2009 and Mercier et al., 2015; or prior analyses of the same dataset in Cappe et al., 2010, 2012). The same statistical design was applied to all ERP measures and source estimations.

To address differential processing according to inter-quartile variability of RTs and presentation condition (i.e., intra-individual variability), 2 x 2 repeated measures ANOVAs with the factors of quartile (first versus fourth) and condition (V and AV) were performed. Note that this analysis was structured to specifically contrast brain responses during trials in which there was evidence for multisensory facilitation exceeding probability summations (first quartile of the RT distribution) from those in which no evidence for such race model violations was found (fourth quartile). The choice of limiting our analyses to contrasting AV and V trials only was motivated by the facts that: 1) adding auditory-only conditions to the statistical design did not significantly alter the results, and 2) by reducing the number of conditions entered into the statistical design matrix, we increased the power in our analyses.

Analyses of the visual and audiovisual ERP waveforms (see Figure 3a for ERPs at a representative midline occipital electrode) as a function of time revealed a main effect of quartile (i.e. intra-subject RT variability) starting at 188ms post-stimulus onset (see Figure 3b). Additionally, there was a significant quartile by condition interaction starting at 184ms post-stimulus onset. Analyses of inter-subject differences (i.e. ANCOVA) revealed a three-way interaction between quartile, condition and between-subject differences in RT spread (i.e. IQR) starting at 196ms and 284ms and post-stimulus onset. These analyses of the ERP waveforms highlight significant differences found at single electrodes over time and serve as an initial indicator of differential neural processing. Nonetheless, these statistical results are reference-dependent and cannot distinguish between activity differences due to changes in response strength from those due to differences in the topographic configuration of the scalp potentials; the latter of which is indicative of a change in the underlying neuronal generators (Murray et al., 2008).

Thus, to quantify statistical differences over the entire electrode montage, we analyzed both global field power (GFP) and topographic dissimilarity (DISS) (Brunet et al., 2011; Michel et al., 2004; Murray et al., 2008). GFP analyses did not reveal any statistically reliable differences. In contrast, the DISS analyses revealed a significant main effect of RT difference (from 142ms - 239ms post-stimulus onset; see Figure 3c). Further, we found a significant IQR by condition interaction at 93ms – 155ms post-stimulus onset, as well as at a subsequent time period (253ms - 280ms). Next, we sought to determine whether these topographic effects stemmed from stable differences in map configurations in each condition, or from latency shifts of map onsets between conditions. To this end, we entered the group-averaged ERPs into an AAHC analysis (Murray et al., 2008). The procedure identified 17 maps that could account for 95.7% of the variance over the four group-averaged ERPs (i.e., AV and V conditions resulting in fast and slow responses) over the entire post-stimulus onset time period. These template maps are shown in Figure 4. During the 183 - 250ms post-stimulus onset period, three maps (framed in black, light gray, and dark gray in Figure 4) differentially characterized group averaged ERPs across conditions.

This pattern observed at the group-averaged ERP level was next statistically assessed in the single-subject ERPs using a spatial-correlation fitting procedure over the 183-250ms post-stimulus period, using within-subject factors of condition (AV and V), RT quartile (slow and fast), and map (Murray et al., 2008). We observed a significant condition × map interaction ($F_{(2,14)}$=11.38; p<0.001; η_p^2=0.62). No other main effect or interaction was statistically reliable (p's>0.10). Given this interaction, we then performed separate ANOVAs for the AV and V conditions. For the AV condition, there was a non-significant trend for a main effect of map ($F_{(2,14)}$=3.65; p=0.053; η_p^2=0.34), but neither main effect of RT quartile nor the interaction was statistically reliable (p's>0.10). This suggests that one template map (i.e. that framed in black) predominated the responses to the AV conditions irrespective of the resultant RT and that the patterns were statistically indistinguishable for responses leading to slow and fast RTs. For the V condition neither main effect was statistically reliable, yet there was a significant interaction between RT quartile and map ($F_{(2,14)}$=5.53; p=0.017; η_p^2=0.44). Post-hoc analyses revealed that for the visual-only condition leading to slow responses, the template map framed in dark grey predominated. By contrast, for the visual-only condition leading to fast responses, the template map framed in light gray predominated. In accordance with our behavioral findings showing a significant reduction of response variability under multisensory conditions, these results revealed a single stable map configuration (and by extension likely a stable neuronal generator configuration) underpinning multisensory processing within the 183ms – 250ms post-stimulus onset window. In addition to quantifying the total duration of a given template map, the fitting procedure also provided output concerning the first onset of a given template map. Analysis of this output indicated an earlier switch between template maps to occur for visual-only presentations resulting in faster RTs than slower RTs (304ms versus 319ms; p-value < 0.001).

Source estimations

The time-window revealed by this clustering analysis (i.e. 183ms – 250ms post-stimulus onset) served as basis for determining the time-window of analysis for the source estimations. Source estimations were carried out in order to identify the networks likely contributing to the effects observed at the scalp level. While the topographic clustering analyses revealed the presence of two distinct template maps under visual-only presentation conditions, one template map predominated the responses under audiovisual conditions. Nonetheless, we chose to collapse over the whole period of interest when computing source estimations. This choice was mainly motivated by our relatively small sample size (*N*=8) and to increase the signal-to-noise ratio of our scalp recordings.

During the time period of interest identified by the clustering procedure (183ms - 250ms post-stimulus onset), all four conditions (i.e. fast and slow responses for visual and audiovisual conditions) included prominent sources within occipital and temporal cortices. Statistical analyses revealed a main effect of RT quartile (i.e. fast versus slow responses) that included several clusters located within bilateral inferior frontal gyrus, the right parietal cortex and the right superior occipital cortex extending to the middle temporal cortex (see Figure 5a and Table 1 for more detailed description). Further analyses revealed a distinct network showing a significant quartile by condition interaction which included sources within the right IFG, right middle frontal gyrus, right superior temporal gyrus, as well as a cluster within left posterior PC (see Figure 5b). There was also a significant three-way interaction between quartile, condition and RT difference located within frontal cortex, extending from the superior frontal cortex to the medial frontal gyrus (see Figure 5c).

Cluster correlations

In a final step, we sought to shed light on the patterns of functional connectivity (in terms of correlated activations) within the brain network showing differential responses as a function of RTs. To this end, we first extracted mean activity across all voxels within the cluster in the left visual areas showing the greatest activity (i.e., 2 standard deviations above the mean activity of whole brain activity) during the 183ms - 250ms post-stimulus onset window (see Methods and Materials). Second, we extracted mean activation values across voxels within each of the three clusters that showed a Main Effect of RTs within the same period of interest (see prior section). Subsequently, we computed student t-values of Spearman's rank-ordered correlation coefficients over time. Due to the relatively small sample size, the reliability of the correlation coefficients was assessed using bootstrap estimations (2000 samples). Subsequently, we estimated differences in correlated activity patterns between visual cortices and the three clusters revealed by the Main Effect of RTs. This analysis sought to extend prior hemodynamic imaging results suggesting differential connectivity within a very similar neuronal network (including visual cortices) to be associated with differences in RTs (see Noppeney et al., 2010). More precisely, correlations were computed as a function of time between the mean cluster activity within left visual cortices (i.e. the cluster showing the greatest activity) and the three clusters identified by the statistical analyses in the source space (i.e. the Main Effect of RTs): 1) a cluster containing the right Angular Gyrus (AG), extending to the posterior Middle Temporal Gyrus (MTG), 2) a cluster in the right inferior Parietal Lobule extending to the superior Occipital Cortex (SOC), and 3) a cluster within the right inferior Frontal Gyrus (IFG).

Correlations between occipital cortices and the three clusters investigated here were significantly less pronounced under multisensory presentation conditions (within the 183ms – 250ms post-stimulus onset time-window). In contrast, response speed under visual-only presentations was facilitated when activity within occipital cortices was correlated with activity within all three clusters (see Figure 6a.i).

In a last step, we sought to further elucidate how the connectivity between nodes beyond visual cortices differentially contributed to RT variability. To do this, we directly correlated activity from each of the three clusters shown to be differentially recruited as a function as RTs with one another (see Figure 6a.ii). Again, we computed t-values of Spearman's rank-ordered correlation coefficients (bootstrap estimation with 2000 samples; time-window 183ms – 250ms; statistical criteria: $t_{(6)}>2.44$; $p<0.05$; >12 contiguous time frames). These analyses showed that during the 183ms – 250ms time-period, inter-cluster correlations between the Angular Gyrus and the inferior parietal lobule were most robust for those conditions that led to faster RTs (i.e. AV fast, AV slow, and V fast; see Figure 6a.ii). Similarly, only trials resulting in fast responses within each condition revealed significant correlations between all three clusters.

Generally, when participants' RTs were fastest (i.e. in under audiovisual presentation conditions), occipital cortices did not exhibit significant correlation with the posterior parietal lobule and the IFG. In contrast, these clusters showed significant activity correlations with occipital cortices, with increased RTs (i.e. under slow responses to audiovisual stimuli and both visual-only presentations). We tentatively hypothesize that this difference in correlation patterns reflects more efficient stimulus processing (i.e., a decrease of the necessity of sustained functional connectivity) between visual cortices and the identified network clusters. In terms of between-cluster correlations, the data clearly showed that faster responses to both audiovisual and visual-only conditions were supported by stronger between cluster activity correlations within the higher-level network (i.e. not including lower-level visual cortices).

Discussion

The current study provides an important link between behavioral and neural data focused on examining intra- and inter-individual differences (i.e., variability) in multisensory processing. The behavioral data support the presence of multisensory integrative processes as evidenced by violations of the race model; a result consistent with a number of prior studies (e.g. Mercier et al., 2015; Pomper, Brincker, Harwood, Prikhodko, & Senkowski, 2014; Sperdin et al., 2009; Stevenson, Fister, Barnett, Nidiffer, & Wallace, 2012). In addition, the behavioral analyses illustrate a reduction in response variability in audiovisual trials, again consistent with prior work (Sarko, Ghose, & Wallace, 2013). Analyses of the scalp recorded EEG data show that differences in RT variability between visual and audiovisual conditions are related to the presence of different stable ERP topographies. Specifically, these analyses revealed the recruitment of a single stable topography to occur under multisensory conditions (which characterized both fast and slow responses). In contrast, two stable network configurations characterized visual-only trials where a greater RT distribution variability was observed. We hypothesize that this apparent stability in the ERP topography under multisensory presentations reflects the more efficient (faster and less variable) processing of audiovisual stimuli. Source estimations suggest that the intra-individual (trial-by-trial) RT variability observed at the behavioral level is linked to differences in the recruitment of an extensive cortical network, which includes occipital, parietal and frontal cortices. Additionally, the analyses suggest that inter-individual differences in the variability of RT distributions can be related to activity within middle frontal cortices. Finally, correlational analyses between clusters within this network revealed that greater behavioral benefits (under both visual and multisensory conditions) appear linked to more correlated (i.e., more efficient) interactions within the clusters of this network. In what follows, we discuss these findings within the framework of the existing literature.

In the current study, our measure of intra- and inter-individual response variability is the mean difference in RTs between the first and the fourth quartiles of the individual RT distributions. These results provide strong evidence that RTs under multisensory conditions are less variable when compared to unisensory visual conditions (for similar results see Altieri & Hudock, 2014; Zehetleitner, Ratko-Dehnert, & Müller, 2015), and are of interest in the context of recent work that has distinguished between the concepts of sensory integration and cue interactions (Otto & Mamassian, 2012). Under circumstances of cue interactions, there should be an accompanying increase in sensory noise from a stimulus in a second modality, thus resulting in a broadening of RT distributions under multisensory conditions in tasks like those used in the current study. In contrast, our observation of a less variable response distribution under multisensory conditions argues for a decrease in sensory noise, suggestive of an active integration process between the visual and auditory cues and supporting concepts of cue reliability (Ernst & Banks, 2002; Morgan, DeAngelis, & Angelaki, 2008).

To date, only a few studies have directly investigated the neuronal loci and networks that are associated with variability in behavioral responses to multisensory stimuli (Noppeney et al., 2010; Sperdin et al., 2009; Tyll et al., 2013). Sperdin and colleagues (2009), reexamining a previously published data set from Murray and colleagues (2005) stemming from an audiotactile detection task, specifically addressed the neuronal interactions that accompanied response time facilitations under multisensory versus unisensory conditions, but did not specifically address the neuronal correlates of RT variability under multisensory conditions. In particular, these authors found a facilitation of RTs under multisensory conditions and that was associated with differences in activation strength over the left posterior superior temporal cortex. Nonetheless their analyses focused only on testing differences in non-linear multisensory interactions as a function of RTs, rather than specifically addressing the neuronal correlates of RT variability per se.

Our findings also help to bridge results from electroencephalography with those from hemodynamic imaging (Noppeney et al., 2010; Tyll et al., 2013). We provide the first evidence that trial-to-trial RT variability within an individual subject is linked to quantitative differences in terms of correlated activity within an occipital-to-frontal network. It has been argued that such correlations of neuronal activity can be highly informative about the functional connectivity (FC) between (relatively) distant cortical regions (Salinas & Sejnowski, 2001). Compared to simple correlation analyses, functional connectivity measures represent a more detailed analysis of the cross-correlation patterns between neural nodes as a function of experimental conditions (see Friston, 2011 for a review). The present results suggest the existence of a strong correlational relationship between the amount of neural activity within this occipito-to-frontal network and both presentation condition (i.e. audiovisual versus visual-only) and response speed (i.e. fast versus slow responses). Moreover, significant changes in activity correlations between neural nodes have been linked back to trial-by-trial fluctuations (i.e. intra-individual performance variability) reflected in behavior (e.g. Hansen, Chelaru, & Dragoi, 2012). Further investigations are needed to provide more detailed information concerning the links between connectivity patterns and their relationship to neural activation patterns and behavioral variability.

Although the current study focused on intra-individual RT variability, our analyses also revealed an important relationship between the neural correlates of intra-individual differences and inter-individual variability. A distinct cluster within frontal cortices exhibited differential activation patterns as a function of response speed (fast versus slow trials), presentation condition (visual-only versus multisensory) and the individual, within-subject RT differences (see Figure 2b). Activity within these areas has been linked to task difficulty and cognitive control mechanisms (Desai, Conant, Waldron, & Binder, 2006; Ridderinkhof, Ullsperger, Crone, & Nieuwenhuis, 2004) and sensory evidence accumulation in decision related processes (Filimon, Philiastides, Nelson, Kloosterman, & Heekeren, 2013; Heekeren, Marrett, & Ungerleider, 2008). Here frontal areas showed stronger activations when subject's RT was slower under multisensory conditions, suggestive of less efficient evidence accumulation as compared to trials resulting in faster responses. Middle frontal areas have been related to individual differences in RT observed in attentional tasks and to aspects of behavioral control (Kelly, Uddin, Biswal, Castellanos, & Milham, 2008; Simmonds et al., 2007). Similarly, it has been suggested that the recruitment of premotor circuits is linked to more efficient behavioral performance (Ionta, Ferretti, Merla, Tartaro, & Romani, 2010; Simmonds et al., 2007), similar to what we have observed for visual-only trials and that resulted in shorter RTs. In other words, previous studies propose that frontal cortices are more strongly recruited under conditions of greater sensory uncertainty and higher cognitive demands. We propose that this increased activity within frontal cortices could reflect greater effort to maintain performance (see Stuss et al., 1989 for a similar proposal; see Figure 6b for an illustration). Stated a bit differently, differential recruitment of frontal areas is linked to inter-individual differences in the ability to maintain performance throughout the task. Such variability across individuals has been linked to differences in the maturation of executive functions as well as personality traits in both clinical and healthy cohorts (Alvarez & Emory, 2006; Barkley, 1997; Stuss, 1992). Thus, our results extend these prior findings by partially dissociating neuronal activation patterns responsible for intra-individual response variability from those related to between-subject differences in response times.

Conclusions

The current behavioral and electrical neuroimaging data provides important insights into the spatiotemporal dynamics involved in RT variability in response to visual-only and audiovisual stimuli. Our results show that RT variability is related to differences in correlated activity of a distributed network involving occipital, temporal, parietal and frontal cortices. Furthermore, our data suggest that the significant reduction of trial-to-trial variability under audiovisual presentations is related to the differential activation of superior and medial frontal cortex, and which account for differences in RTs as a function of race model predictions (i.e. violation versus non-violation). In contrast, for visual-only trials a more extensive occipito-to-frontal network must be considered to explain RT variability.

Acknowledgements

The STEN toolbox (http://www.unil.ch/line/home/menuinst/about-the-line/software--analysis-tools.html) has been programmed by Jean-François Knebel, from the Laboratory for Investigative Neurophysiology (the LINE), Lausanne, Switzerland, and is supported by the Center for Biomedical Imaging (CIBM) of Geneva and Lausanne and by National Center of Competence in Research project “SYNAPSY – The Synaptic Bases of Mental Disease”; project no. 51AU40_125759. Support for MMM is from the Swiss National Science Foundation (grants 320030-149982 and 320030_169206) and from a grantor advised by Carigest SA. Support for AT is from the Swiss National Science Foundation (grant numbers P2LAP3_151771 and P300PB_164754). Support for SI is from the Swiss National Science Foundation (grant PZ00P1_148186 and PP00P1_170506/1) and by the International Foundation for Research in Paraplegia (grant P164). Support for MTW is from NIH (grant numbers HD083211 and MH109225).

References

Altieri, N., & Hudock, D. (2014). Hearing impairment and audiovisual speech integration ability: a case study report. *Frontiers in Psychology*, *5*(July), 678. https://doi.org/10.3389/fpsyg.2014.00678

Altieri, N., Stevenson, R. A., Wallace, M. T., & Wenger, M. J. (2015). Learning to Associate Auditory and Visual Stimuli: Behavioral and Neural Mechanisms. *Brain Topography*, *28*(3), 479–493. https://doi.org/10.1007/s10548-013-0333-7

Alvarez, J. A., & Emory, E. (2006). Executive Function and the Frontal Lobes: A Meta-Analytic Review. *Neuropsychology Review*, *16*(1), 17–42. https://doi.org/10.1007/s11065-006-9002-x

Barkley, R. A., & A., R. (1997). Behavioral inhibition, sustained attention, and executive functions: Constructing a unifying theory of ADHD. *Psychological Bulletin*, *121*(1), 65–94. https://doi.org/10.1037/0033-2909.121.1.65

Bellgrove, M. A., Hester, R., & Garavan, H. (2004). The functional neuroanatomical correlates of response variability: evidence from a response inhibition task. *Neuropsychologia*, *42*(14), 1910–6. https://doi.org/10.1016/j.neuropsychologia.2004.05.007

Bourgeois, A., Chica, A. B., Valero-Cabré, A., & Bartolomeo, P. (2013). Cortical control of inhibition of return: causal evidence for task-dependent modulations by dorsal and ventral parietal regions. *Cortex; a Journal Devoted to the Study of the Nervous System and Behavior*, *49*(8), 2229–38. https://doi.org/10.1016/j.cortex.2012.10.017

Brunet, D., Murray, M. M., & Michel, C. M. (2011). Spatiotemporal analysis of multichannel EEG: CARTOOL. *Computational Intelligence and Neuroscience*, *2011*, 813870. https://doi.org/10.1155/2011/813870

Cappe, C., Thelen, A., Romei, V., Thut, G., & Murray, M. M. (2012). Looming signals reveal synergistic principles of multisensory integration. *Journal of Neuroscience*, *32*(4), 1171–1182. https://doi.org/10.1523/JNEUROSCI.5517-11.2012

Cappe, C., Thut, G., Romei, V., & Murray, M. M. (2009). Selective integration of auditory-visual looming cues by humans. *Neuropsychologia*, *47*(4), 1045–52. https://doi.org/10.1016/j.neuropsychologia.2008.11.003

Cappe, C., Thut, G., Romei, V., & Murray, M. M. (2010). Auditory-visual multisensory interactions in humans: timing, topography, directionality, and sources. *The Journal of Neuroscience : The Official Journal of the Society for Neuroscience*, *30*(38), 12572–80. https://doi.org/10.1523/JNEUROSCI.1099-10.2010

Castellanos, F. X., Sonuga-Barke, E. J. S., Scheres, A., Di Martino, A., Hyde, C., & Walters, J. R. (2005). Varieties of attention-deficit/hyperactivity disorder-related intra-individual variability. *Biological Psychiatry*, *57*(11), 1416–23. https://doi.org/10.1016/j.biopsych.2004.12.005

Chaumon, M., & Busch, N. A. (2014). Prestimulus neural oscillations inhibit visual perception via modulation of response gain. *Journal of Cognitive Neuroscience*, *26*(11), 2514–29. https://doi.org/10.1162/jocn_a_00653

Corbetta, M., & Shulman, G. L. (2002). Control of goal-directed and stimulus-driven attention in the brain. *Nature Reviews. Neuroscience*, *3*(3), 201–15. https://doi.org/10.1038/nrn755

de Graaf, T. a, Gross, J., Paterson, G., Rusch, T., Sack, A. T., & Thut, G. (2013). Alpha-band rhythms in visual task performance: phase-locking by rhythmic sensory stimulation. *PloS One*, *8*(3), e60035. https://doi.org/10.1371/journal.pone.0060035

Dehaene, S. (1993). Temporal oscillations in human perception. *Psychological Science*, *4*(4), 264–270. https://doi.org/10.1111/j.1467-9280.1993.tb00273.x

Delorme, A., & Makeig, S. (2004). EEGLAB: an open source toolbox for analysis of single-trial EEG dynamics including independent component analysis. *Journal of Neuroscience Methods*, *134*(1), 9–21. https://doi.org/10.1016/j.jneumeth.2003.10.009

Desai, R., Conant, L. L., Waldron, E., & Binder, J. R. (2006). fMRI of Past Tense Processing: The Effects of Phonological Complexity and Task Difficulty. *Journal of Cognitive Neuroscience*, *18*(2), 278–297. https://doi.org/10.1162/jocn.2006.18.2.278

Dickman, S. (1985). Impulsivity and perception: individual differences in the processing of the local and global dimensions of stimuli. *Journal of Personality and Social Psychology*, *48*(1), 133–49.

Ernst, M. O., & Banks, M. S. (2002). Humans integrate visual and haptic information in a statistically optimal fashion. *Nature*, *415*(6870), 429–433. https://doi.org/10.1038/415429a

Filimon, F., Philiastides, M. G., Nelson, J. D., Kloosterman, N. A., & Heekeren, H. R. (2013). How embodied is perceptual decision making? Evidence for separate processing of perceptual and motor decisions. *The Journal of Neuroscience : The Official Journal of the Society for Neuroscience*, *33*(5), 2121–36. https://doi.org/10.1523/JNEUROSCI.2334-12.2013

Fiske, D. W., & Rice, L. (1955). Intra-individual response variability. *Psychological Bulletin*, *52*(3), 217–50.

Fründ, I., Busch, N. A., Schadow, J., Körner, U., & Herrmann, C. S. (2007). From perception to action: phase-locked gamma oscillations correlate with reaction times in a speeded response task. *BMC Neuroscience*, *8*(1), 27. https://doi.org/10.1186/1471-2202-8-27

Gingras, G., Rowland, B. A., & Stein, B. E. (2009). The differing impact of multisensory and unisensory integration on behavior. *The Journal of Neuroscience : The Official Journal of the Society for Neuroscience*, *29*(15), 4897–902. https://doi.org/10.1523/JNEUROSCI.4120-08.2009

Gonzalez Andino, S. L., Murray, M. M., Foxe, J. J., & de Peralta Menendez, R. G. (2005). How single-trial electrical neuroimaging contributes to multisensory research. *Experimental Brain Research. Experimentelle Hirnforschung. Expérimentation Cérébrale*, *166*(3–4), 298–304. https://doi.org/10.1007/s00221-005-2371-1

Grave de Peralta Menendez, R., Gonzalez Andino, S., Lantz, G., Michel, C. M., & Landis, T. (2001). Noninvasive localization of electromagnetic epileptic activity. I. Method descriptions and simulations. *Brain Topography*, *14*(2), 131–7.

Grave de Peralta Menendez, R., Murray, M. M., Michel, C. M., Martuzzi, R., & Gonzalez Andino, S. L. (2004). Electrical neuroimaging based on biophysical constraints. *NeuroImage*, *21*(2), 527–39. https://doi.org/10.1016/j.neuroimage.2003.09.051

Grill-Spector, K. (2003). The neural basis of object perception. *Current Opinion in Neurobiology*, *13*(2), 159–166. https://doi.org/10.1016/S0959-4388(03)00040-0

Guthrie, D., & Buchwald, J. S. (1991). Significance testing of difference potentials. *Psychophysiology*, *28*(2), 240–4.

Hansen, B. J., Chelaru, M. I., & Dragoi, V. (2012). Correlated variability in laminar cortical circuits. *Neuron*, *76*(3), 590–602. https://doi.org/10.1016/j.neuron.2012.08.029

Heekeren, H. R., Marrett, S., & Ungerleider, L. G. (2008). The neural systems that mediate human perceptual decision making. *Nature Reviews. Neuroscience*, *9*(6), 467–79. https://doi.org/10.1038/nrn2374

Iacoboni, M., & Zaidel, E. (2003). Interhemispheric visuo-motor integration in humans: the effect of redundant targets. *The European Journal of Neuroscience*, *17*(9), 1981–6.

Ionta, S., Ferretti, A., Merla, A., Tartaro, A., & Romani, G. L. (2010). Step-by-step: the effects of physical practice on the neural correlates of locomotion imagery revealed by fMRI. *Human Brain Mapping*, *31*(5), 694–702. https://doi.org/10.1002/hbm.20898

Ivanov, I., & Werner, A. (n.d.). Colour in action: Evidence for a redundancy signal effect when driving motor responses by combined colour and spatial cues.

Kanai, R., & Rees, G. (2011). The structural basis of inter-individual differences in human behaviour and cognition. *Nature Reviews. Neuroscience*, *12*(4), 231–42. https://doi.org/10.1038/nrn3000

Kane, M. J., & Engle, R. W. (2002). The role of prefrontal cortex in working-memory capacity, executive attention, and general fluid intelligence: an individual-differences perspective. *Psychonomic Bulletin & Review*, *9*(4), 637–671. https://doi.org/10.3758/BF03196323

Kelly, A. M. C., Uddin, L. Q., Biswal, B. B., Castellanos, F. X., & Milham, M. P. (2008). Competition between functional brain networks mediates behavioral variability. *NeuroImage*, *39*(1), 527–37. https://doi.org/10.1016/j.neuroimage.2007.08.008

Koenig, T., Kottlow, M., Stein, M., & Melie-García, L. (2011). Ragu: a free tool for the analysis of EEG and MEG event-related scalp field data using global randomization statistics. *Computational Intelligence and Neuroscience*, *2011*, 938925. https://doi.org/10.1155/2011/938925

Krummenacher, J., Grubert, A., Töllner, T., & Müller, H. J. (2014). Salience-based integration of redundant signals in visual pop-out search: evidence from behavioral and electrophysiological measures. *Journal of Vision*, *14*(3), 26. https://doi.org/10.1167/14.3.26

Lopez-Calderon, J., & Luck, S. J. (2014). ERPLAB: an open-source toolbox for the analysis of event-related potentials. *Frontiers in Human Neuroscience*, *8*, 213. https://doi.org/10.3389/fnhum.2014.00213

Los, S. A., & Van der Burg, E. (2013). Sound speeds vision through preparation, not integration. *Journal of Experimental Psychology. Human Perception and Performance*, *39*(6), 1612–24. https://doi.org/10.1037/a0032183

MacDonald, S. W. S., Nyberg, L., & Bäckman, L. (2006). Intra-individual variability in behavior: links to brain structure, neurotransmission and neuronal activity. *Trends in Neurosciences*, *29*(8), 474–480. https://doi.org/10.1016/j.tins.2006.06.011

Martuzzi, R., Murray, M. M., Maeder, P. P., Fornari, E., Thiran, J.-P., Clarke, S., … Meuli, R. A. (2006). Visuo-motor pathways in humans revealed by event-related fMRI. *Experimental Brain Research*, *170*(4), 472–87. https://doi.org/10.1007/s00221-005-0232-6

Martuzzi, R., Murray, M. M., Meuli, R. A., Thiran, J.-P., Maeder, P. P., Michel, C. M., … Gonzalez Andino, S. L. (2009). Methods for determining frequency- and region-dependent relationships between estimated LFPs and BOLD responses in humans. *Journal of Neurophysiology*, *101*(1), 491–502. https://doi.org/10.1152/jn.90335.2008

Mercier, M. R., Molholm, S., Fiebelkorn, I. C., Butler, J. S., Schwartz, T. H., & Foxe, J. J. (2015). Neuro-oscillatory phase alignment drives speeded multisensory response times: an electro-corticographic investigation. *The Journal of Neuroscience : The Official Journal of the Society for Neuroscience*, *35*(22), 8546–57. https://doi.org/10.1523/JNEUROSCI.4527-14.2015

Michel, C. M., Murray, M. M., Lantz, G., Gonzalez, S., Spinelli, L., & Grave de Peralta, R. (2004). EEG source imaging. *Clinical Neurophysiology : Official Journal of the International Federation of Clinical Neurophysiology*, *115*(10), 2195–222. https://doi.org/10.1016/j.clinph.2004.06.001

Miller, J. (1982). Divided attention: evidence for coactivation with redundant signals. *Cognitive Psychology*, *14*(2), 247–279. https://doi.org/10.1016/0010-0285(82)90010-X

Miller, J., & Ulrich, R. (2003). Simple reaction time and statistical facilitation: a parallel grains model. *Cognitive Psychology*, *46*(2), 101–51.

Miniussi, C., Girelli, M., & Marzi, C. A. (1998). Neural site of the redundant target effect electrophysiological evidence. *Journal of Cognitive Neuroscience*, *10*(2), 216–30.

Morell, L., & Morell, F. (1966). Evoked Potentials and Reaction TImes: A study of intra-individual variability. *Electroencephalography and Clinical Neurophysiology*, *20*, 567–575.

Morgan, M. L., DeAngelis, G. C., & Angelaki, D. E. (2008). Multisensory Integration in Macaque Visual Cortex Depends on Cue Reliability. *Neuron*, *59*(4), 662–673. https://doi.org/10.1016/j.neuron.2008.06.024

Murray, M. M., Brunet, D., & Michel, C. M. (2008). Topographic ERP analyses: a step-by-step tutorial review. *Brain Topography*, *20*(4), 249–64. https://doi.org/10.1007/s10548-008-0054-5

Murray, M. M., Foxe, J. J., Higgins, B. A., Javitt, D. C., & Schroeder, C. E. (2001). Visuo-spatial neural response interactions in early cortical processing during a simple reaction time task: a high-density electrical mapping study. *Neuropsychologia*, *39*(8), 828–44.

Murray, M. M., Molholm, S., Michel, C. M., Heslenfeld, D. J., Ritter, W., Javitt, D. C., … Foxe, J. J. (2004). Grabbing Your Ear: Rapid Auditory-Somatosensory Multisensory Interactions in Low-level Sensory Cortices Are Not Constrained by Stimulus Alignment. *Cerebral Cortex*, *15*(7), 963–974. https://doi.org/10.1093/cercor/bhh197

Murray, M. M., & Wallace, M. T. (Eds.) (2011). The Neural Bases of Multisensory Processes. CRC Press/Taylor & Francis Group. Boca Roton, FL.

Noppeney, U., Ostwald, D., & Werner, S. (2010). Perceptual decisions formed by accumulation of audiovisual evidence in prefrontal cortex. *The Journal of Neuroscience : The Official Journal of the Society for Neuroscience*, *30*(21), 7434–46. https://doi.org/10.1523/JNEUROSCI.0455-10.2010

Oldfield, R. C. (1971). The assessment and analysis of handedness: the Edinburgh inventory. *Neuropsychologia*, *9*(1), 97–113.

Otto, T. U., Dassy, B., & Mamassian, P. (2013). Principles of multisensory behavior. *The Journal of Neuroscience : The Official Journal of the Society for Neuroscience*, *33*(17), 7463–74. https://doi.org/10.1523/JNEUROSCI.4678-12.2013

Otto, T. U., & Mamassian, P. (2012). Noise and correlations in parallel perceptual decision making. *Current Biology : CB*, *22*(15), 1391–6. https://doi.org/10.1016/j.cub.2012.05.031

Peelen, M. V, & Downing, P. E. (2007). The neural basis of visual body perception. *Nature Reviews. Neuroscience*, *8*(8), 636–48. https://doi.org/10.1038/nrn2195

Pérez-Bellido, A., Soto-Faraco, S., & López-Moliner, J. (2013). Sound-driven enhancement of vision: disentangling detection-level from decision-level contributions. *Journal of Neurophysiology*, *109*(4), 1065–77. https://doi.org/10.1152/jn.00226.2012

Perrin F, Pernier J, Bertrand O, Giard MH, E. J., Perrin, F., Pernier, J., Bertrand, O., Giard, M. H., & Echallier, J. F. (1987). Mapping of scalp potentials by surface spline interpolation. *Electroencephalography and Clinical Neurophysiology*, *66*(1), 75–81.

Pomper, U., Brincker, J., Harwood, J., Prikhodko, I., & Senkowski, D. (2014). Taking a call is facilitated by the multisensory processing of smartphone vibrations, sounds, and flashes. *PloS One*, *9*(8), e103238. https://doi.org/10.1371/journal.pone.0103238

Pulvermüller, F., & Fadiga, L. (2010). Active perception: sensorimotor circuits as a cortical basis for language. *Nature Reviews. Neuroscience*, *11*(5), 351–60. https://doi.org/10.1038/nrn2811

Ratcliff, R. (1993). Methods for dealing with reaction time outliers. *Psychological Bulletin*, *114*(3), 510–32.

Ridderinkhof, K. R., Ullsperger, M., Crone, E. A., & Nieuwenhuis, S. (2004). The role of the medial frontal cortex in cognitive control. *Science (New York, N.Y.)*, *306*(5695), 443–7. https://doi.org/10.1126/science.1100301

Romei, V., Gross, J., & Thut, G. (2010). On the Role of Prestimulus Alpha Rhythms over Occipito-Parietal Areas in Visual Input Regulation: Correlation or Causation?, *30*(25), 8692–8697. https://doi.org/10.1523/JNEUROSCI.0160-10.2010

Salinas, E., & Sejnowski, T. J. (2001). Correlated neuronal activity and the flow of neural information. *Nature Reviews Neuroscience*, *2*(8), 539–550. https://doi.org/10.1038/35086012

Sarko, D. K., Ghose, D., & Wallace, M. T. (2013). Convergent approaches toward the study of multisensory perception. *Frontiers in Systems Neuroscience*, *7*, 81. https://doi.org/10.3389/fnsys.2013.00081

Saron, C. D., Schroeder, C. E., Foxe, J. J., & Vaughan, H. G. (2001). Visual activation of frontal cortex: segregation from occipital activity. *Brain Research. Cognitive Brain Research*, *12*(1), 75–88.

Schmid, M. C., & Maier, A. (2015). To see or not to see--thalamo-cortical networks during blindsight and perceptual suppression. *Progress in Neurobiology*, *126*, 36–48. https://doi.org/10.1016/j.pneurobio.2015.01.001

Senkowski, D., Molholm, S., Gomez-Ramirez, M., & Foxe, J. J. (2006). Oscillatory beta activity predicts response speed during a multisensory audiovisual reaction time task: a high-density electrical mapping study. *Cerebral Cortex (New York, N.Y. : 1991)*, *16*(11), 1556–65. https://doi.org/10.1093/cercor/bhj091

Simmonds, D. J., Fotedar, S. G., Suskauer, S. J., Pekar, J. J., Denckla, M. B., & Mostofsky, S. H. (2007). Functional brain correlates of response time variability in children. *Neuropsychologia*, *45*(9), 2147–57. https://doi.org/10.1016/j.neuropsychologia.2007.01.013

Sperdin, H. F., Cappe, C., Foxe, J. J., Murray, M. M., & Neuroscience, I. (2009). Early, low-level auditory-somatosensory multisensory interactions impact reaction time speed. *Frontiers in Integrative Neuroscience*, *3*(March), 1–10. https://doi.org/10.3389/neuro.07

Sperdin, H. F., Cappe, C., & Murray, M. M. (2010). The behavioral relevance of multisensory neural response interactions. *Frontiers in Neuroscience*, *4*, 9. https://doi.org/10.3389/neuro.01.009.2010

Stevenson, R. a, Fister, J. K., Barnett, Z. P., Nidiffer, A. R., & Wallace, M. T. (2012). Interactions between the spatial and temporal stimulus factors that influence multisensory integration in human performance. *Experimental Brain Research. Experimentelle Hirnforschung. Expérimentation Cérébrale*, *219*(1), 121–37. https://doi.org/10.1007/s00221-012-3072-1

Stuss, D. T. (1992). Biological and psychological development of executive functions. *Brain and Cognition*, *20*(1), 8–23. https://doi.org/10.1016/0278-2626(92)90059-U

Stuss, D. T., Floden, D., Alexander, M. P., Levine, B., & Katz, D. (2001). Stroop performance in focal lesion patients: dissociation of processes and frontal lobe lesion location. *Neuropsychologia*, *39*(8), 771–86.

Stuss, D. T., Murphy, K. J., Binns, M. A., & Alexander, M. P. (2003). Staying on the job: the frontal lobes control individual performance variability. *Brain : A Journal of Neurology*, *126*(Pt 11), 2363–80. https://doi.org/10.1093/brain/awg237

Stuss, D. T., Stethem, L. L., Hugenholtz, H., Picton, T., Pivik, J., & Richard, M. T. (1989). Reaction time after head injury: fatigue, divided and focused attention, and consistency of performance. *Journal of Neurology, Neurosurgery, and Psychiatry*, *52*(6), 742–8. https://doi.org/10.1136/JNNP.52.6.742

Talairach, J., & Tournoux, P. (1988). Co-planar stereotaxic atlas of the human brain. 3-Dimensional proportional system: an approach to cerebral imaging.

Thelen, A., Cappe, C., & Murray, M. M. (2012). Electrical neuroimaging of memory discrimination based on single-trial multisensory learning. *NeuroImage*, *62*(3), 1478–1488. https://doi.org/10.1016/j.neuroimage.2012.05.027

Thelen, A., Matusz, P. J., & Murray, M. M. (2014). Multisensory context portends object memory. *Current Biology*, *24*(16), R734–R735. https://doi.org/10.1016/j.cub.2014.06.040

Toepel, U., Knebel, J.-F., Hudry, J., le Coutre, J., & Murray, M. M. (2009). The brain tracks the energetic value in food images. *NeuroImage*, *44*(3), 967–74. https://doi.org/10.1016/j.neuroimage.2008.10.005

Tyll, S., Bonath, B., Schoenfeld, M. A., Heinze, H.-J., Ohl, F. W., & Noesselt, T. (2013). Neural basis of multisensory looming signals. *NeuroImage*, *65*, 13–22. https://doi.org/10.1016/j.neuroimage.2012.09.056

Ulrich, R., & Miller, J. (1997). Tests of Race Models for Reaction Time in Experiments with Asynchronous Redundant Signals. *Journal of Mathematical Psychology*, *41*(4), 367–81.

Ulrich, R., Miller, J., & Schröter, H. (2007). Testing the race model inequality: An algorithm and computer programs. *Behavior Research Methods*, *39*(2), 291–302. https://doi.org/10.3758/BF03193160

Witkin, H. A. (1949). The nature and importance of individual differences in perception. *Journal of Personality*, *18*(2), 145–70, pl. https://doi.org/10.1111/j.1467-6494.1949.tb01237.x

Witkin, H. A. (1950). Individual differences in ease of perception of embedded figures. *Journal of Personality*, *19*(1), 1–15.

Yarkoni, T., Barch, D. M., Gray, J. R., Conturo, T. E., & Braver, T. S. (2009). BOLD correlates of trial-by-trial reaction time variability in gray and white matter: a multi-study fMRI analysis. *PloS One*, *4*(1), e4257. https://doi.org/10.1371/journal.pone.0004257

Zehetleitner, M., Ratko-Dehnert, E., & Müller, H. J. (2015). Modeling violations of the race model inequality in bimodal paradigms: co-activation from decision and non-decision components. *Frontiers in Human Neuroscience*, *9*, 119. https://doi.org/10.3389/fnhum.2015.00119

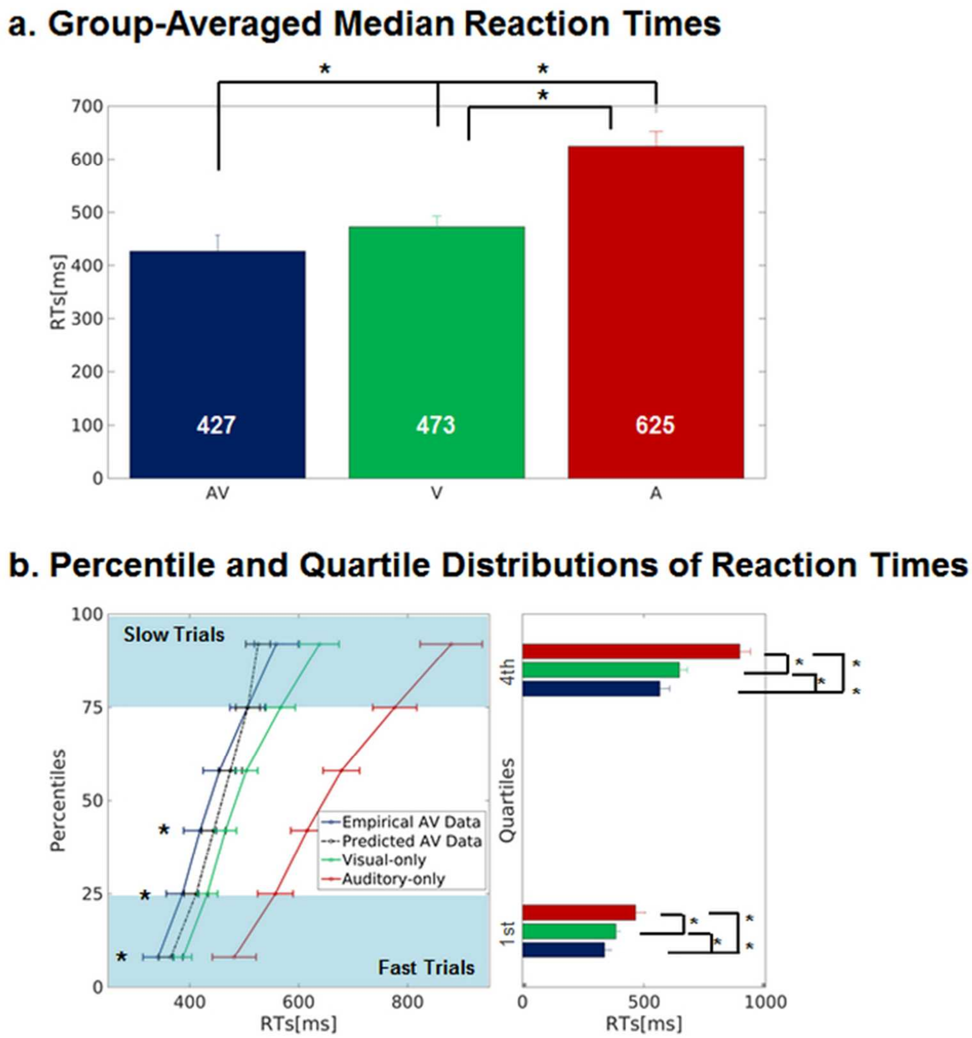

Figure 1. Group-averaged reaction times (RTs). a. Median RTs for multisensory (blue), visual-only (green) and auditory-only (red) conditions. b. Left column: Cumulative distribution functions derived from the RTs. The dashed black line represents the predicted RTs from the Race Model. The actual RT distributions are shown for multisensory (blue), visual-only (green) and auditory-only (red) conditions. The light blue bars highlight the first and the last quartiles of the distribution. Right column: Group-averaged median RTs for the multisensory (blue), visual-only (green) and auditory-only (red) conditions of the first and forth quartile. Asterisks indicate significant differences. Error bars represent the standard error of the mean (SEM).

60x64mm (300 x 300 DPI)

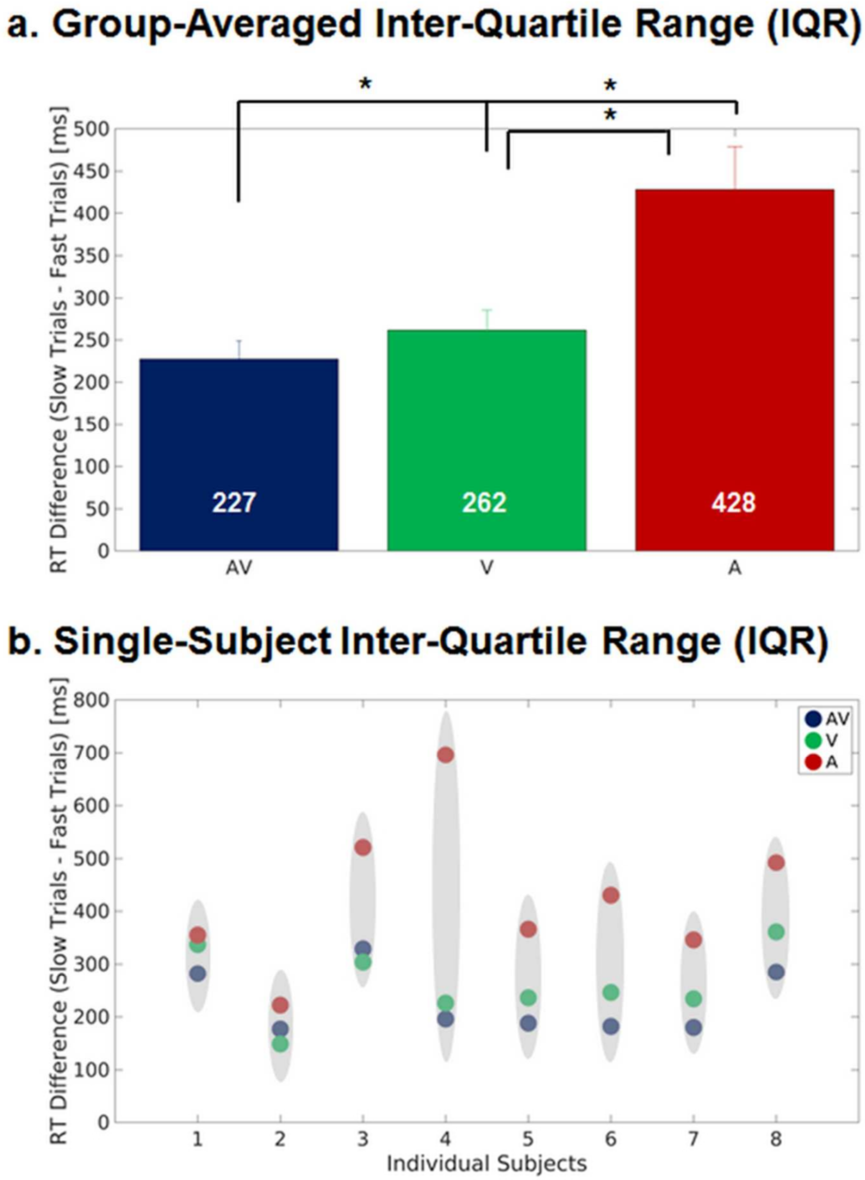

Figure 2. Inter-quartile reaction time differences. a. Group-averaged inter-quartile ranges (IQRs) between the first and the fourth quartiles of the cumulative distribution functions for each condition. Asterisks indicate significant (p<0.05) differences between all conditions. Error bars represent the SEM. b. The RT difference between quartiles for each individual subject. The dots indicate the difference of median RT for each subject for the multisensory (blue), visual-only (green) and auditory-only conditions.

60x77mm (300 x 300 DPI)

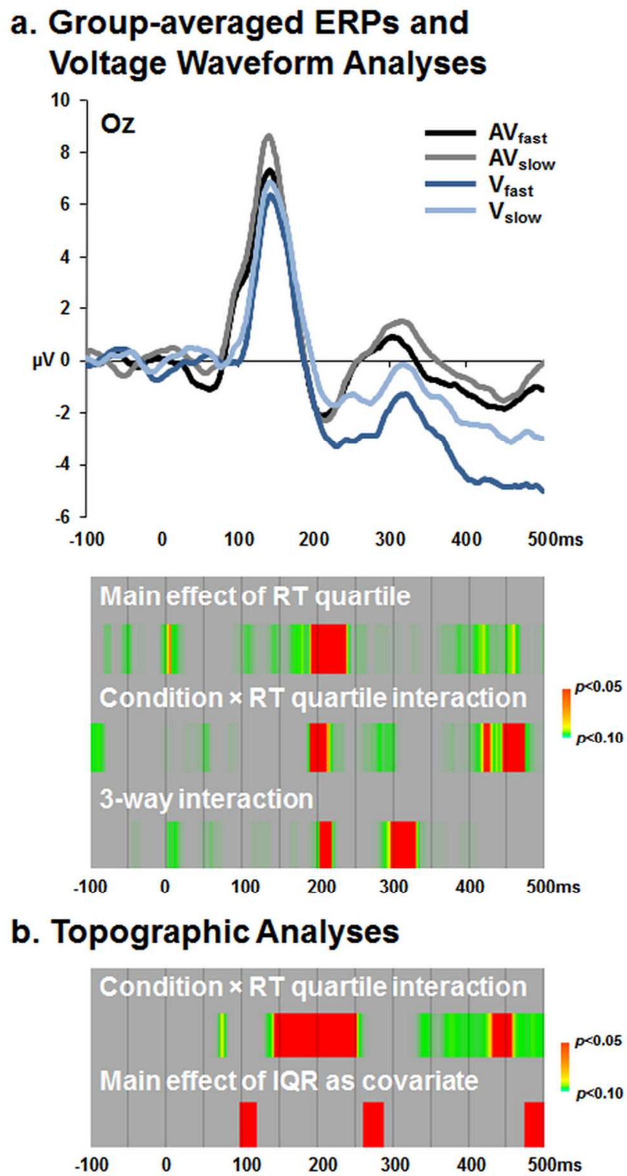

Figure 3. Exemplar group-averaged event-related potentials (ERPs) as well as results of voltage waveform and topographic analyses. a. Group-averaged ERP waveforms from an exemplar midline occipital electrode (Oz) for the fast and slow multisensory (black and gray) as well as fast and slow visual-only (dark and light blue) conditions are shown. Below are the results of the ANCOVA analysis at each electrode that was performed at each time frame. Only effects persisting in time (>11ms consecutively) and space (>5% of the electrode montage) were considered reliable (shown in red). b. Results from the ANCOVA analysis using Global Map Dissimilarity.

60x110mm (300 x 300 DPI)

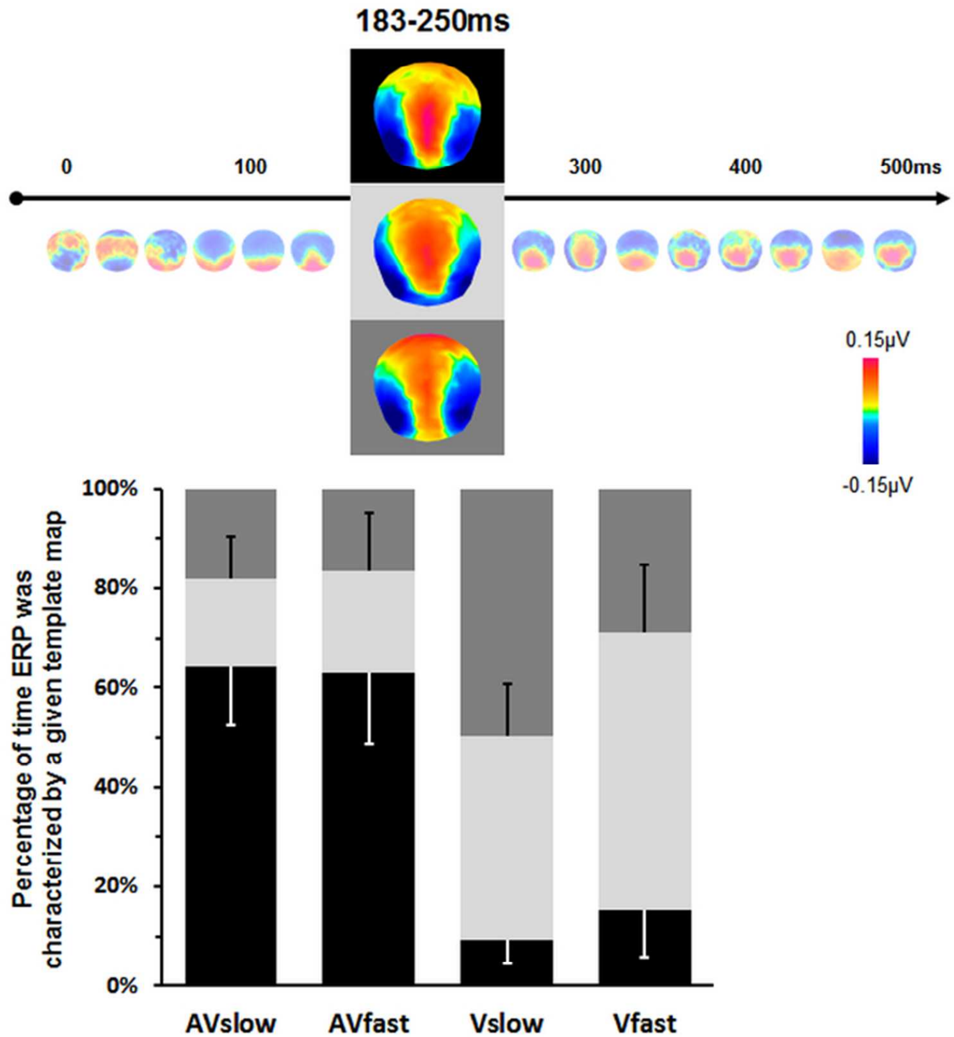

Figure 4. Results from the topographic agglomerative hierarchical clustering (AAHC) analyses are shown. a. Template maps from the AAHC analysis. During the 500ms post-stimulus onset period 17 maps explained 96% of the variance of the data (i.e. audiovisual fast and slow responses, visual-only fast and slow responses). Three maps appeared to differentially account for audiovisual (black framed map) and visual-only (light and dark gray maps) conditions over the 183-250ms post-stimulus period. b. The results of the fitting procedure are displayed in the bar graph, which indicates the percentage of time that each template map characterized each ERP over the 183-250ms period. The black-framed map predominated responses to the AV condition irrespective of RT speed, whereas different and distinct template maps predominated unisensory responses as a function of RT speed.

60x65mm (300 x 300 DPI)

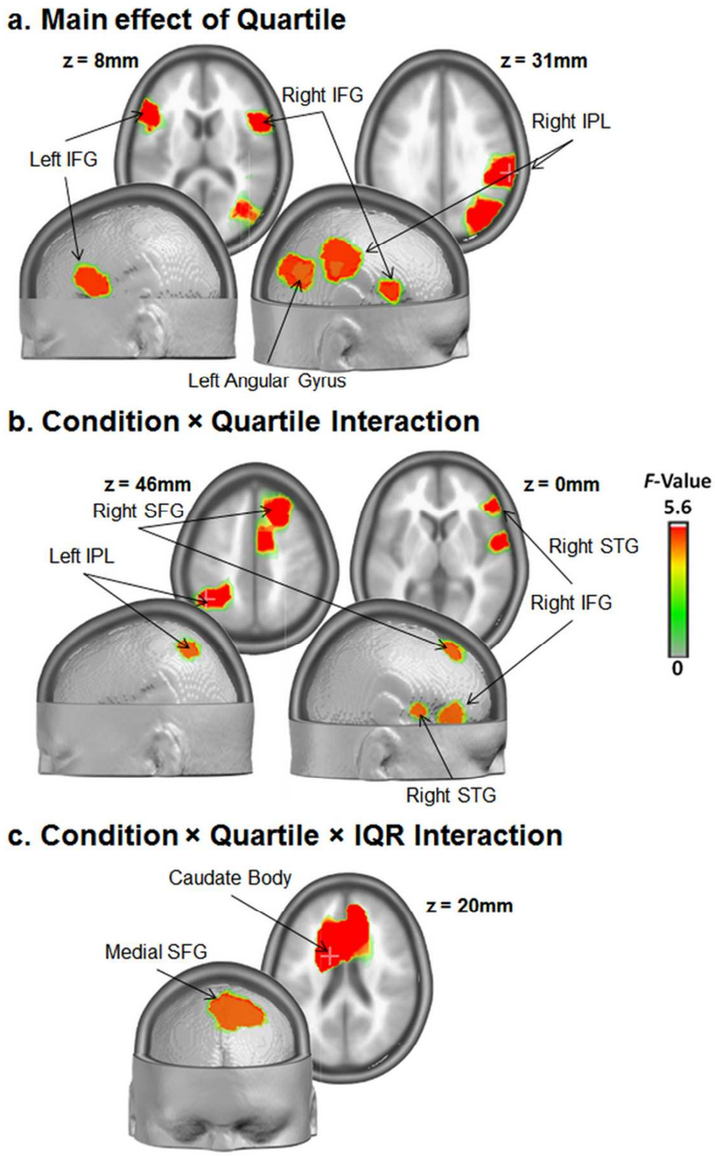

Figure 5. The results from the 2×2 ANOVA on source estimations (averaged over the 183-250ms post-stimulus onset period) are shown. Only results satisfying the statistical threshold of $p<0.05$ and $k_E>12$nodes are shown (coordinates of maximal F-values indicated below). a. The main effect of RT quartile yielded four clusters: the IFG bilaterally (left= -50, 19, 8mm; right= 54, 13, 8mm), the right parietal cortex (64, -32, 31mm) and the right superior occipital cortex extending to the middle temporal cortex (44, -68, 28mm). b. Clusters exhibiting a significant condition × quartile interaction included the right IFG (52, 31, -1mm), the right MFG (26, 30, 48mm), the right STG (57, 2, 0mm), and the left PPC (-46, -51, 46mm). c. A single cluster within the superior frontal cortex extending downwards and medially exhibited a significant three-way interaction (-14, 6, 20mm).

60x97mm (300 x 300 DPI)

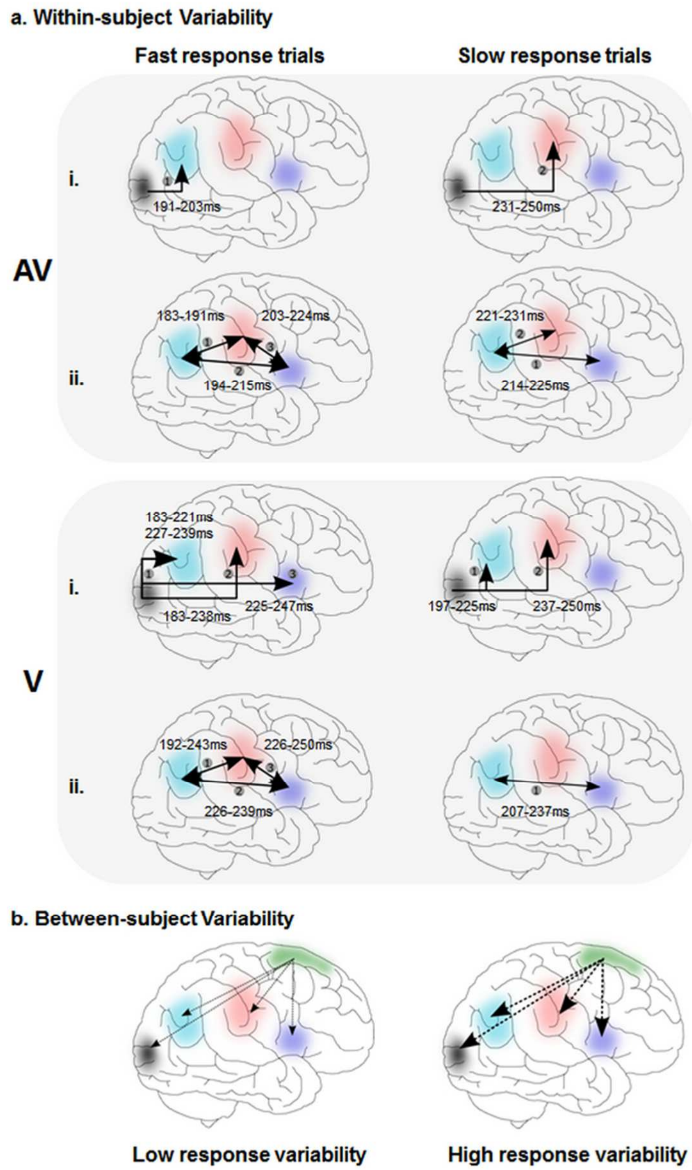

Figure 6. Presumptive models of the differences in connectivity and strength of connectivity between the experimental conditions and their relationship to within-subject (a) and between-subject (b) connectivity. The representations are constructed based largely on the cluster correlation analyses. Columns depict the results as a function of fast (left) versus slow (right) response trials, and are divided based on AV (top) versus V (bottom) conditions. The rows labeled i. depict the correlation analyses between occipital cortices (black) and clusters identified by the main effect of quartile including the right angular gyrus (light blue), the right posterior parietal lobule (red) and the inferior frontal gyrus (purple). The rows labeled ii. depict the between-cluster correlations of these three nodes. The model illustrated in b. is derived from the results of the between-subject analyses as a function of response variability (ANCOVA). We hypothesize that greater activity within superior medial frontal cortices (green) as a function of individual RT variability further modulates activity patterns within the three nodes of interest.

60x97mm (300 x 300 DPI)